Online Supplement

Title

Mice lacking hypertension candidate gene ATP2B1 in vascular smooth muscle cells show significant blood pressure elevation

Authors

Yusuke Kobayashi[1)], Nobuhito Hirawa[2)], Yasuharu Tabara[3)], Hidenori Muraoka[4)], Megumi Fujita[1)], Nobuko Miyazaki[1)], Akira Fujiwara[1)], Yasuhiro Ichikawa[5)], Yuichiro Yamamoto[2)], Naoaki Ichihara[1)], Sanae Saka[1)], Hiromichi Wakui[1)], Shin-ichiro Yoshida[1)], Keisuke Yatsu[2)], Yoshiyuki Toya[1)], Gen Yasuda[2)], Katsuhiko Kohara[3)], Yoshikuni Kita[6)], Kohtaro Takei[4)], Yoshio Goshima[4)], Yoshihiro Ishikawa[5)], Hirotsugu Ueshima[6)], Tetsuro Miki[3)], Satoshi Umemura[1)]

Affiliations

1. Department of Medical Science and Cardiorenal Medicine, Yokohama City University Graduate School of Medicine, Yokohama, Japan
2. Division of Nephrology and Hypertension, Yokohama City University Medical Center, Yokohama, Japan
3. Department of Geriatric Medicine, Ehime University Graduate School of Medicine, Toon, Japan
4. Department of Molecular Pharmacology and Neurobiology, Yokohama City University Graduate School of Medicine, Yokohama, Japan
5. Cardiovascular Research Institute, Yokohama City University Graduate School of Medicine, Yokohama, Japan
6. Department of Health Science, Shiga University of Medical Science, Otsu, Japan

METHODS

Animal Care

Animals were housed under a 12-hour day/night cycle at a temperature of 25°C. Tap water was provided *ad libitum*. Experiments were conducted under the guidelines for animal experiments set by the Animal Experiment Committee of Yokohama City University School of Medicine. In order to clarify the importance of the ATP2B1 gene in blood pressure regulation, we attempt to knock out the function of the ATP2B1 gene

of vascular smooth muscle cells. To generate conditional ATP2B1 KO mice, we utilized the Cre-loxP and FLP-FRT recombination system.

Cre-Mice

SM22-Cre mice [Tg(Tagln-cre)1Her/J, stock #004746] were obtained from The Jackson Laboratory (Bar Harbor, ME, USA). The SM22-Cre transgenic mice express Cre recombinase under control of the mouse transgelin (smooth muscle protein 22-alpha) promoter. Thus SM22-Cre mice knockout the gene that is sandwiched with loxP sites in vascular smooth muscle cell (VSMC) specifically. Mice engineered in this study were backcrossed onto the (C57BL/6J) genetic background for at least six generations.

ATP2B1 conditional knockout (KO) mouse

Conditional ATP2B1 KO mouse was generated by Cre/loxP and FLP-FRT recombination system. ATP2B1 is encoded by 21 exons on chromosome 10, and mice lacking exon 10 was reported to be an embryonic lethal. We therefore designed a new vector to knockout the exon 10 of ATP2B1 gene (Figure S1). This targeting vector contains a loxP-FRT-PGK-neo-FRT cassette with 5,572 bp of ATP2B1 homologous regions upstream of exon 10, and loxP site with 3,891 bp homologous regions downstream of exon 10. After linearization and electroporation into the C57BL/6 (RENKA) ES cell lines (Transgenic Inc., Kumamoto, Japan), 431 neo-resistant ES cell clones were obtained. Among the randomly selected 143 ES clones, homologous recombination was confirmed in six clones (#73583, #73584, #73588, #73612, #73693, #73697) by KpnI or PvuII digested Southern blot analysis using 5' probe, 3' probe or neo probe (Figure S2, S3, S4). To verify the recombination of loxP site downstream exon 10, PCR-amplified fragment length (using primer A and primer B) was analyzed by agarose-gel electrophoresis (Figure S5). Both wild-type allele (460 bp) and mutant allele (519 bp) was ascertained in all six clones. We next eliminated the PGK-neo region by transfection of Flp recombinase vector in to the #73588 clone (Figure S6). Flp/FRT recombination was verified by analyzing the length of PCR product amplified with primer C and primer D (Figure S7). Among 104 transfected clones, recombination was ascertained in the seven clones (#77743, #77775, #77936, #77937, #77956, #77961, #77964). KpnI or EcoRI digested Southern blot analysis using 5' probe, 3' probe, or DR probe further confirmed the Flp/FRT recombination in all seven clones (Figure S8). Three ATP2B1floxed ES cell clones (#77743, #77775, #77936) were aggregated with 8-cell stage embryos (ICR strain). The embryo was transferred into uterus of recipient females, and chimeras were delivered by Caesarean section at embryonic 17 day. The

chimeras were mated with wild-type mouse, and germline transmission was ascertained in 14 (9 male, and 5 female) of 31 F1 mouse.

Creation of the Vascular Smooth Muscle Cell-targeted ATP2B1 KO Mice

ATP2B1$^{loxP/loxP}$ mice were generated by the Cre-loxP and FLP-FRT recombination system. ATP2B1 is encoded by 21 exons on chromosome 10, and mice lacking exon 10 are reported to be embryo-lethal. We therefore designed a vector to knockout exon 10 of the ATP2B1 gene. To target inactivation of the ATP2B1 gene to VSMC, ATP2B1$^{loxP/loxP}$ mice were intercrossed with SM22-Cre transgenic mice expressing Cre recombinase under control of the mouse transgelin (smooth muscle protein 22-alpha) promoter. The resulting ATP2B1$^{loxP/-}$/SM22-Cre animals were further mated with ATP2B1$^{loxP/loxP}$ mice to generate ATP2B1$^{loxP/loxP}$/SM22-Cre (VSMC ATP2B1 KO) mice and ATP2B1$^{loxP/loxP}$ mice without SM22-Cre (control mice). Animals used for experiments were backcrossed at least 6 times.

Blood Pressure Measured by Radiotelemetric Method

Direct blood pressure measurement was performed by a radiotelemetric method in which a blood pressure transducer (PA-C10, Data Sciences International, USA) was inserted into the left carotid artery. Ten days after transplantation, each mouse was housed individually in a standard cage on a receiver under a 12-hour light-dark cycle. Direct blood pressure was recorded every minute by radiotelemetry, as described previously [1].

Cell Culture of Mouse VSMC

The VSMC were aseptically isolated from thoracic aortic explants of an 8-week-old ATP2B1 KO mouse and its wild-type littermate as described previously [2]. VSMC were prepared by the explant method and cultured in Dulbecco's modified Eagle's Medium as described previously [3, 4]. VSMC multiplying in a medium containing FBS rapidly lose their contractile features and become "synthetic" cells [3]. Thus, the early passage cells (third to sixth passage) were used in the present study. Subconfluent VSMC were used in the following experiments. The serum of these cells were deprived for 24 hours and then stimulated as indicated. After the desired incubation period, cells were rinsed with ice-cold phosphate-buffered saline and then lysed and sonicated.

Western Blot Analysis of ATP2B1

Western blot analysis was performed as described previously [5, 6]. Briefly, tissue extracts

were used for electrophoresis, and membranes (Millipore, USA) were incubated with rabbit polyclonal anti-ATP2B1 antibody (MBL, Japan) and subjected to enhanced chemiluminescence (GE Healthcare, US). The images were analyzed quantitatively using a FUJI LAS3000 Image Analyzer (FUJI Film, Japan) for determination of the ATP2B1 protein level. To measure the aortic expression ratio of ATP2B1/β-actin, each ATP2B1 protein level was divided by the corresponding β-actin protein level obtained by re-probing, and thus derived from the same extract.

Isometric Tension of the Femoral Artery Vascular Rings

After the mice were anesthetized with pentobarbital, the femoral artery ring was isolated and placed in a tissue bath and kept at 37° C. Two tungsten wires (40 μm in diameter) were threaded into the lumen, and the preparation was mounted in a two-channel myograph (Dual Wire myograph system 410A; Danish Myo Technology, Aarhus, Denmark). One tungsten wire was connected to a micro-manipulator, and the other was connected to a force transducer. All of the vascular rings were initially stabilized for at least 60 min with a modified Krebs-Henseleit solution (Sigma-Aldrich) whose temperature was maintained at 37 °C by a heated water jacket. Isometric tension was continuously monitored using a PowerLab/8 SP system (ADInstruments, Inc., Colorado Springs, CO). After the vascular ring was relaxed, the resting tension was adjusted to 5 mN. After normalization, phenylephrine (Sigma-Aldrich) was added to stimulate vasoconstriction. The concentration of phenylephrine was increased from 10^{-8} M to 10^{-5} M. After a plateau vasoconstriction had been attained, phenylephrine was washed out. At the end of all experiments, vasoconstriction of the femoral artery ring was induced by potassium-enriched solutions containing (in mM): KCl 120, $CaCl_2$ 2.5, $MgSO_4$ 1.17, $NaHCO_3$ 25, KH_2PO_4 1.18, EDTA 0.027, Glucose 5.5.

RESULTS

VSMC ATP2B1 KO Mice showed Higher Blood Pressure Assessed by 24-hour Radiotelemetric System than Control Mice

To confirm the effects of deletion of vascular smooth muscle cell ATP2B1 on blood pressure and to analyze the circadian pattern of blood pressure, conscious VSMC ATP2B1 KO mice and control mice were subjected to blood pressure measurements by radiotelemetry. KO mice showed higher blood pressure than control mice at 14 weeks of age throughout the day (diastolic blood pressure; Figure S9A, mean blood pressure;

Figure S9B).

REFERENCES

1. Mills PA, Huetteman DA, Brockway BP, Zwiers LM, Gelsema AJ, Schwartz RS, Kramer K: A new method for measurement of blood pressure, heart rate, and activity in the mouse by radiotelemetry. *J Appl Physiol.* 2000;88:1537-1544.
2. Kobayashi M, Inoue K, Warabi E, Minami T, Kodama T: A simple method of isolating mouse aortic endothelial cells. *J Atheroscler Thromb.* 2005;12:138-142.
3. Hashimoto T, Kihara M, Sato K, Imai N, Tanaka Y, Sakai M, Tamura K, Hirawa N, Toya Y, Kitamura H, Umemura S: Heparin recovers AT1 receptor and its intracellular signal transduction in cultured vascular smooth muscle cells. *FEBS Lett.* 2005;579:281-284.
4. Hashimoto T, Kihara M, Yokoyama K, Fujita T, Kobayashi S, Matsushita K, Tamura K, Hirawa N, Toya Y, Umemura S: Lipoxygenase products regulate nitric oxide and inducible nitric oxide synthase production in interleukin-1beta stimulated vascular smooth muscle cells. *Hypertens Res.* 2003;26:177-184.
5. Tsurumi Y, Tamura K, Tanaka Y, Koide Y, Sakai M, Yabana M, Noda Y, Hashimoto T, Kihara M, Hirawa N, Toya Y, Kiuchi Y, Iwai M, Horiuchi M, Umemura S: Interacting molecule of AT1 receptor, atrap, is colocalized with AT1 receptor in the mouse renal tubules. *Kidney Int.* 2006;69:488-494.
6. Tanaka Y, Tamura K, Koide Y, Sakai M, Tsurumi Y, Noda Y, Umemura M, Ishigami T, Uchino K, Kimura K, Horiuchi M, Umemura S: The novel angiotensin II type 1 receptor (at1r)-associated protein atrap downregulates at1r and ameliorates cardiomyocyte hypertrophy. *FEBS Lett.* 2005;579:1579-1586.

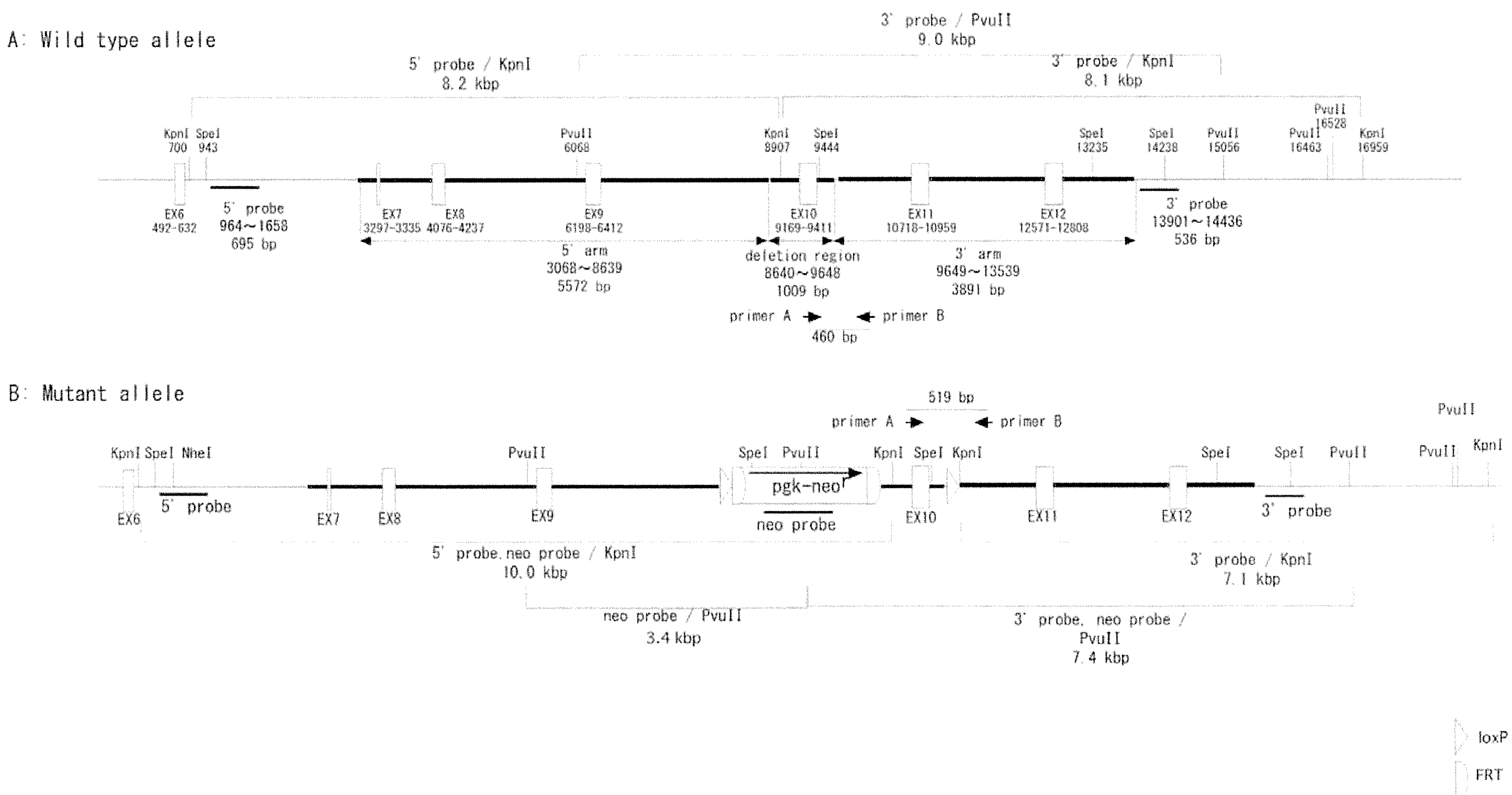
A: Wild type allele
5' probe / KpnI
8.2 kbp
3' probe / PvuII
9.0 kbp
3' probe / KpnI
8.1 kbp
KpnI 700
SpeI 943
PvuII 6068
KpnI 8907
SpeI 9444
SpeI 13235
SpeI 14238
PvuII 15056
PvuII 16463
PvuII 16528
KpnI 16959
EX6 492-632
5' probe 964～1658 695 bp
EX7 3297-3335
EX8 4076-4237
EX9 6198-6412
EX10 9169-9411
EX11 10718-10959
EX12 12571-12808
3' probe 13901～14436 536 bp
5' arm 3068～8639 5572 bp
deletion region 8640～9648 1009 bp
3' arm 9649～13539 3891 bp
primer A
primer B
460 bp
B: Mutant allele
519 bp
primer A
primer B
KpnI SpeI NheI
PvuII
SpeI PvuII
KpnI SpeI KpnI
SpeI
SpeI PvuII
PvuII
PvuII KpnI
pgk-neo
EX6
5' probe
EX7
EX8
EX9
neo probe
EX10
EX11
EX12
3' probe
5' probe, neo probe / KpnI
10.0 kbp
3' probe / KpnI
7.1 kbp
neo probe / PvuII
3.4 kbp
3' probe, neo probe / PvuII
7.4 kbp
loxP
FRT

Figure S1 Vector design of ATP2B1 exon 10 conditional KO mouse

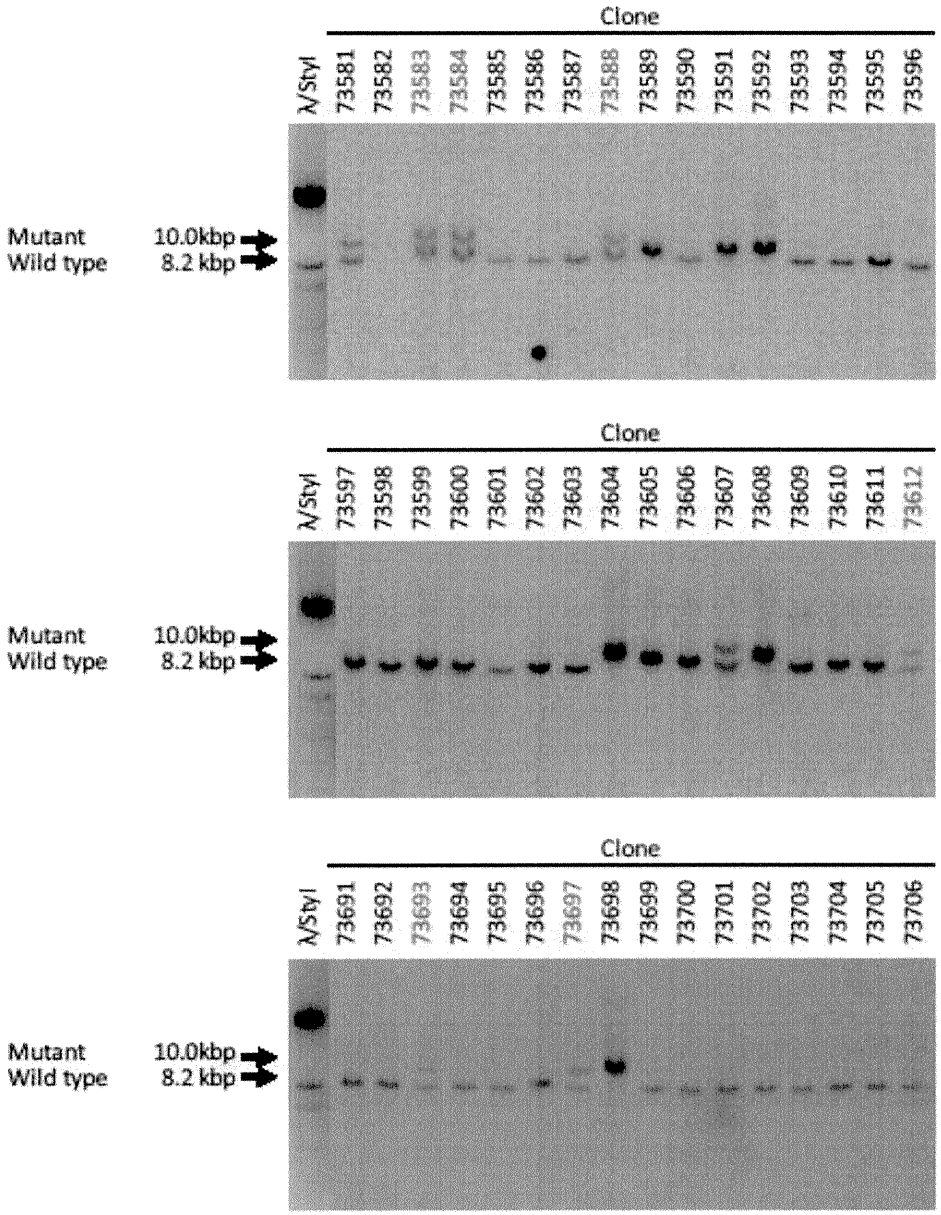

Figure S2 Kpn I-digested Southern blot analysis using 5' probe

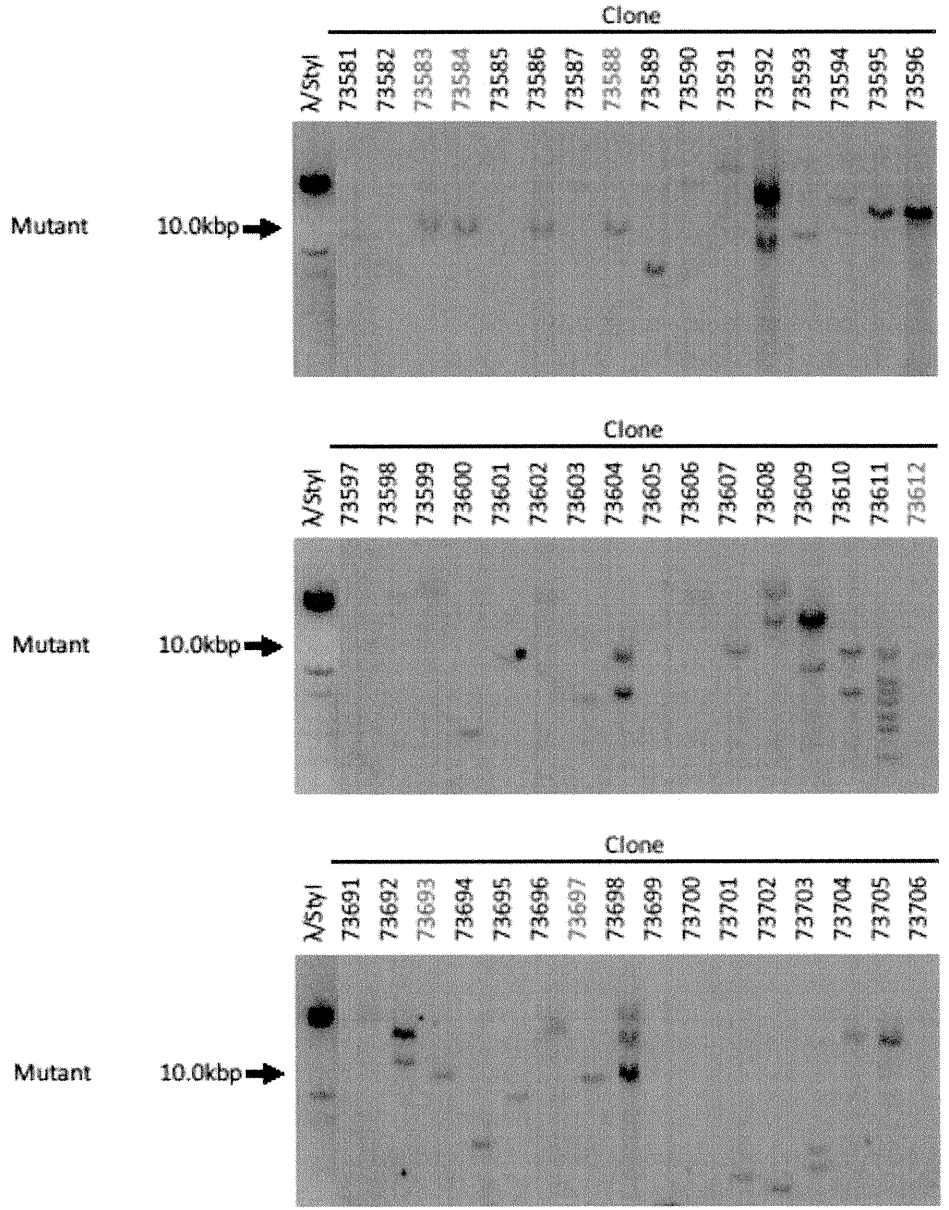

Figure S3 Kpn I-digested Southern blot analysis using neo probe

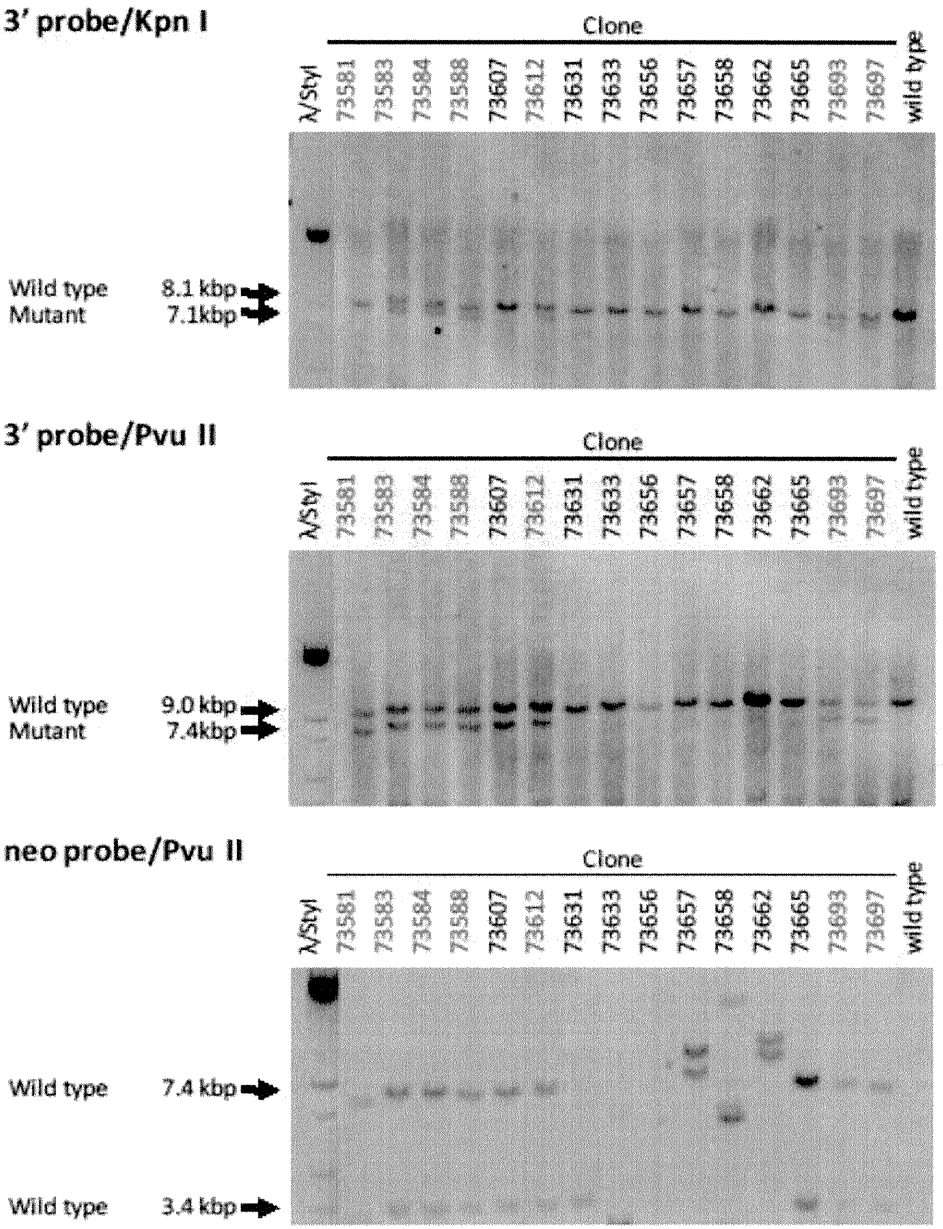

Figure S4 Kpn I/Pvu II-digested Southern blot analysis using 3'/neo probe

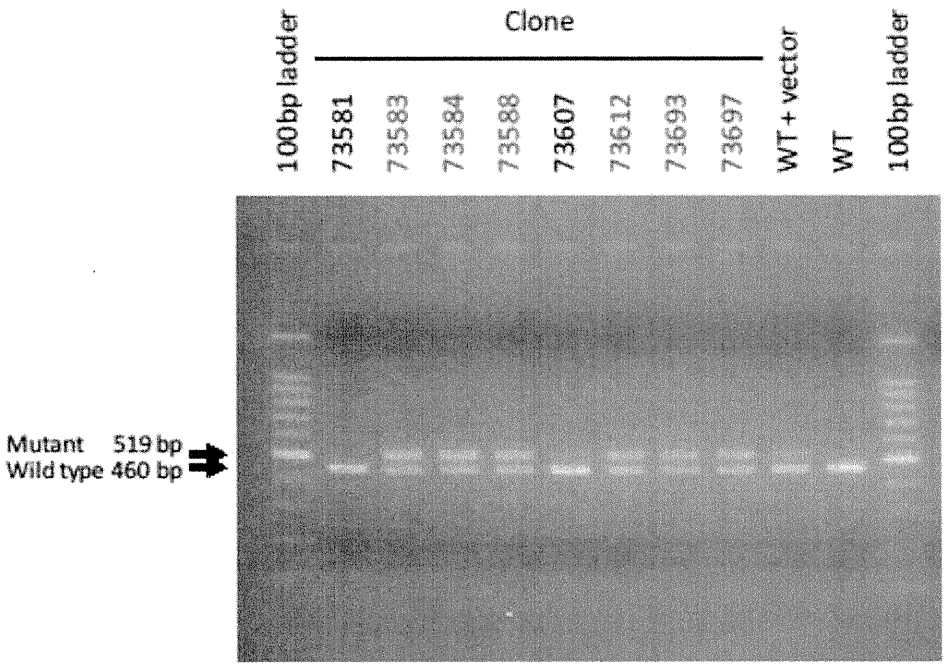

Figure S5 Agarose-gel electrophoresis of PCR products amplified with primer A and primer B

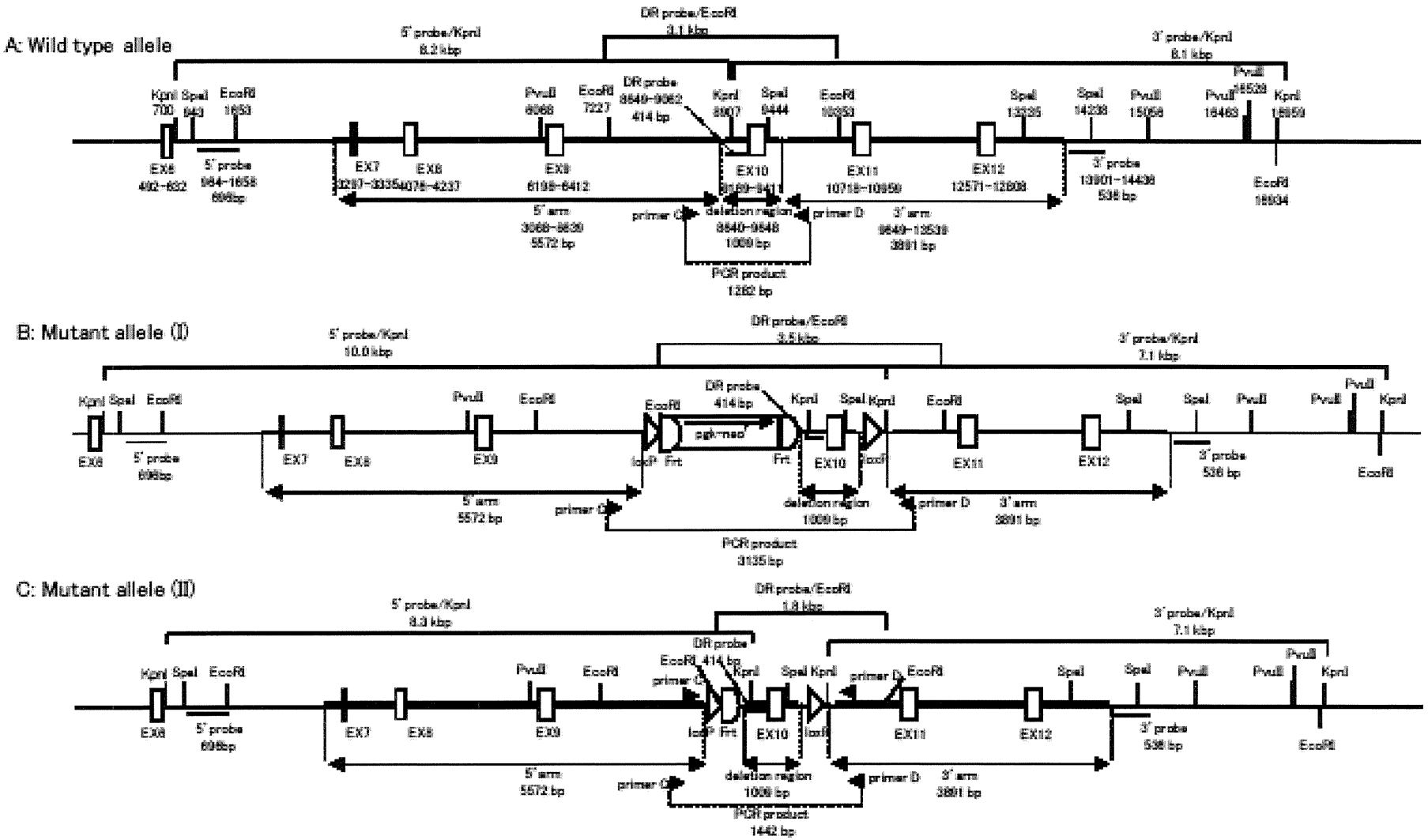

Figure S6 Eliminated the PGK-neo region by Flp recombination system

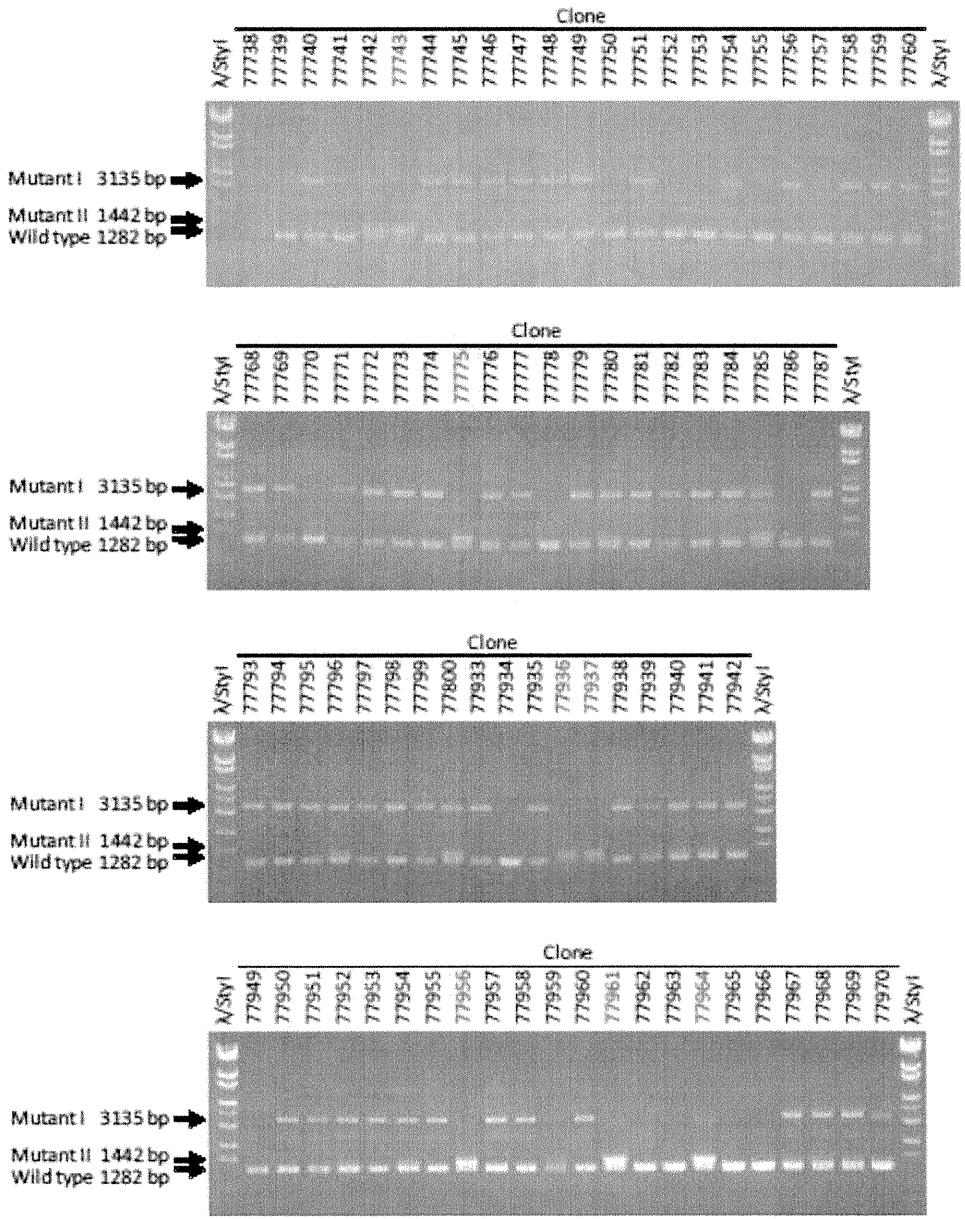

Figure S7 Agarose-gel electrophoresis of PCR products amplified with primer C and primer D

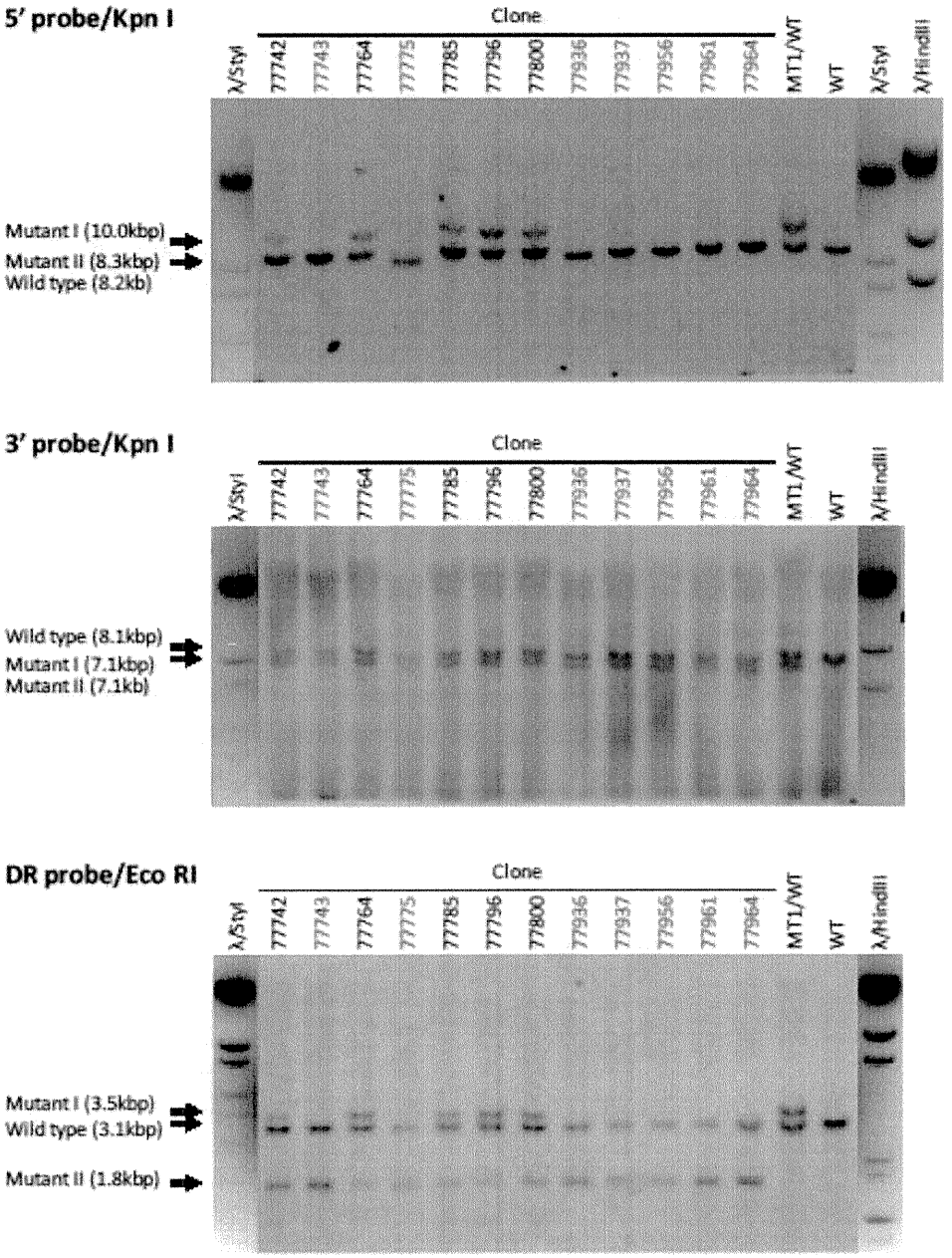

Figure S8 Kpn I/EcoRI-digested Southern blot analysis

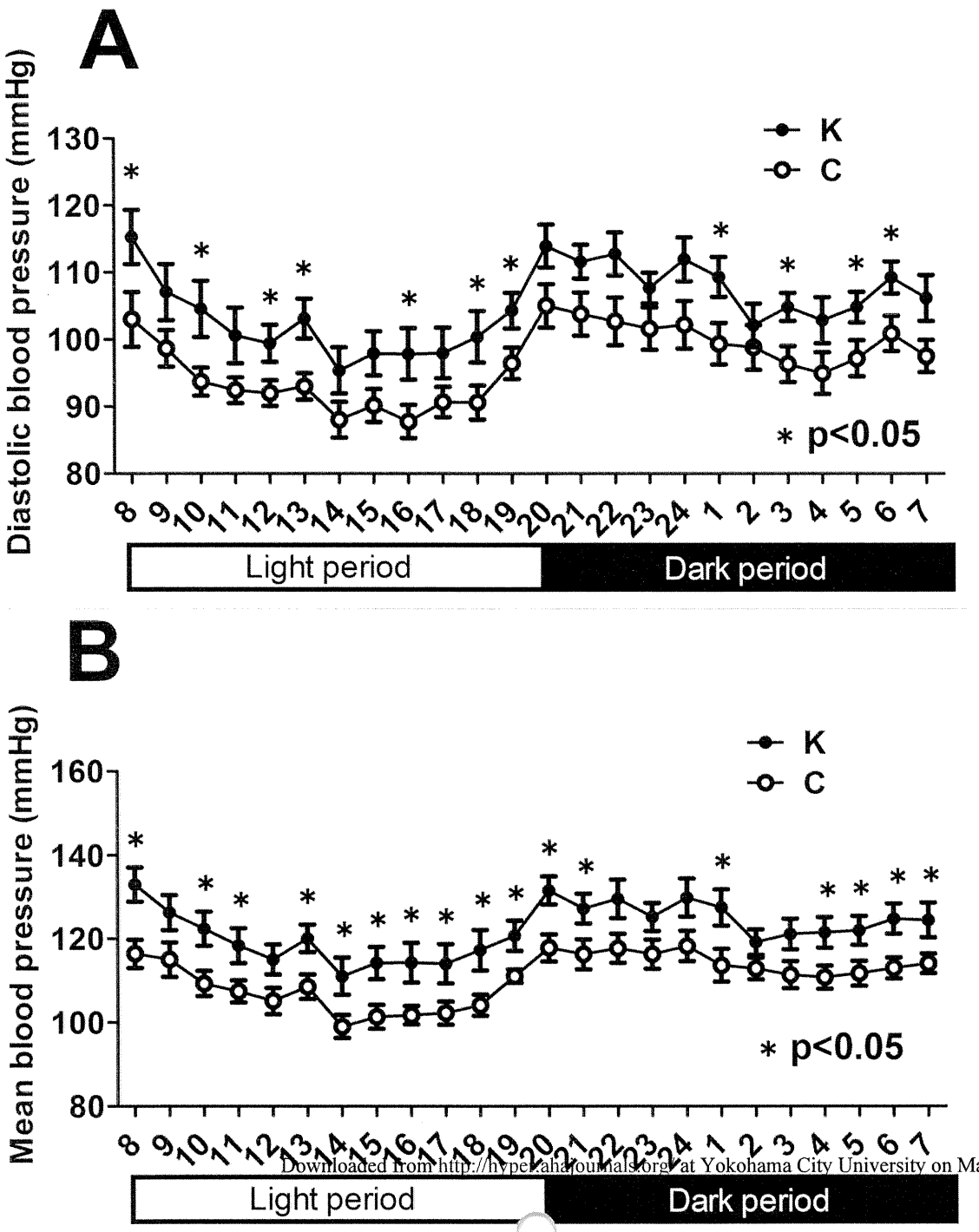

Figure S9 Diastolic and mean blood pressure measured by radiotelemetry

(A) Circadian patterns of diastolic blood pressure in VSMC ATP2B1 KO mice (n=9) and control mice (n=9) on a 12 hour light (8 AM to 8 PM) / dark (8 PM to 8 AM) cycle are shown. Mice were studied on a normal-salt diet. Values plotted are hourly means and standard errors measured over 60 hours (C: control mice, K: VSMC ATP2B1 KO mice). (B) Circadian patterns of mean blood pressure in VSMC ATP2B1 KO mice (n=9) and control mice (n=9) on a 12 hour light (8 AM to 8 PM) / dark (8 PM to 8 AM) cycle are shown. Mice were studied on a normal-salt diet. Values plotted are hourly means and standard errors measured over 60 hours.

THE JOURNAL OF BIOLOGICAL CHEMISTRY VOL. 286, NO. 22, pp. 19682–19692, June 3, 2011
Printed in the U.S.A.

Secretoglobin 3A2 Suppresses Bleomycin-induced Pulmonary Fibrosis by Transforming Growth Factor β Signaling Down-regulation*[S]

Received for publication, March 10, 2011, and in revised form, April 8, 2011 Published, JBC Papers in Press, April 10, 2011, DOI 10.1074/jbc.M111.239046

Reiko Kurotani[‡§¶], Satoshi Okumura[§], Tsutomu Matsubara[‡], Utako Yokoyama[§], John R. Buckley[‡], Takeshi Tomita[‡], Kyohei Kezuka[§], Tomokazu Nagano[‡], Dominic Esposito[‖], Troy E. Taylor[‖], William K. Gillette[‖], Yoshihiro Ishikawa[§], Hiroyuki Abe[¶], Jerrold M. Ward[‡‡], and Shioko Kimura[‡1]**

*From the [‡]Laboratory of Metabolism, NCI, National Institutes of Health, Bethesda, Maryland 20892, the [§]Cardiovascular Research Institute, Yokohama City University, Yokohama, Kanagawa, Japan 236-0004, [¶]Biochemical Engineering, Faculty of Engineering, Yamagata University, Yonezawa, Yamagata, Japan 992-8510, [‖]Protein Expression Laboratory, Advanced Technology Program, SAIC-Frederick, Inc. NCI, National Institutes of Health, Frederick, Maryland 21701, the **Cardiovascular Research Institute, Department of Cell Biology and Molecular Medicine and Medicine (Cardiology), New Jersey Medical School, University of Medicine and Dentistry of New Jersey, Newark, New Jersey 07103, and the [‡‡]Global VetPathology, Montgomery Village, Maryland 20866*

With increasing worldwide rates of morbidity and mortality of pulmonary fibrosis, the development of effective therapeutics for this disease is of great interest. Secretoglobin (SCGB) 3A2, a novel cytokine-like molecule predominantly expressed in pulmonary airways epithelium, exhibits anti-inflammatory and growth factor activities. In the current study SCGB3A2 was found to inhibit TGFβ-induced differentiation of fibroblasts to myofibroblasts, a hallmark of the fibrogenic process, using pulmonary fibroblasts isolated from adult mice. This induction was through increased phosphorylation of STAT1 and expression of SMAD7 and decreased phosphorylation of SMAD2 and SMAD3. To demonstrate the effect of SCGB3A2 on the TGFβ signaling *in vivo*, a bleomycin-induced pulmonary fibrosis mouse model was used. Mice were administered bleomycin intratracheally followed by intravenous injection of recombinant SCGB3A2. Histological examination in conjunction with inflammatory cell counts in bronchoalveolar lavage fluids demonstrated that SCGB3A2 suppressed bleomycin-induced pulmonary fibrosis. Microarray analysis was carried out using RNAs from lungs of bleomycin-treated mice with or without SCGB3A2 and normal mice treated with SCGB3A2. The results demonstrated that SCGB3A2 affects TGFβ signaling and reduces the expression of genes involved in fibrosis. This study suggests the potential utility of SCGB3A2 for targeting TGFβ signaling in the treatment of pulmonary fibrosis.

An increasing number of people are affected by pulmonary fibrosis worldwide, with increasing morbidity and mortality rates. In the United States, the number of patients suffering from pulmonary fibrosis is about 200,000 (1, 2) (www.nhlbi.nih.gov). Recovery from pulmonary fibrosis is possible at early stages of the disease, whereas the recovery is limited once the fibrosis has progressed. A risk for developing pulmonary fibrosis increases by administration of bleomycin (BLM),[2] an anticancer and antibiotic agent, used in therapy for many types of solid tumors.

Fibrosis arises from inflammation initiated by cell injury, and injured tissues are gradually replaced by collagen fibers that are produced from fibroblasts and accumulate as myofibroblasts. Damaged cells produce chemokines, which stimulate leukocytes to proliferate and produce profibrotic cytokines such as transforming growth factor β (TGFβ), a major profibrotic growth factor, and interleukin-13 (IL-13), a major profibrotic mediator. TGFβ1 induces collagen type I transcription through the SMAD signaling, whereas IL-13 stimulates macrophages to produce TGFβ (3–6). On the other hand, interferon-γ (IFNγ) inhibits collagen generation through STAT1 activation followed by sequestration of p300, which plays a pivotal role in the regulation of collagen synthesis by TGFβ (7, 8). IFNγ also induces the antagonistic SMAD7, which in turn impairs TGFβ signaling through inhibition of the SMAD3 interaction with the TGFβ receptor (9) and/or disruption of formation of the TGFβ-induced functional SMAD-DNA complex (10). Other molecules are also involved in the fibrotic process (6). These include other Th2 cytokines such as IL-4, IL-5, and IL-10, chemokines such as CCL2 and CCL3, connective tissue growth factor, and platelet-derived growth factor (3, 11). Molecules involved in various pathways leading to myofibroblast expansion are considered to be useful as therapeutic targets. To this end, a number of inhibitors and/or monoclonal antibodies against these targeted molecules have been developed and subjected to clinical trials as a means to treat fibrosis (3, 11, 12). IFNγ is one of the targeted molecules used as a new therapy for

* This work was supported by the National Institutes of Health, Center for Cancer Research (Intramural Research Program of the NCI; NIH 0010190305 and Z01 BC010449-06, to S. K.). This work was also supported by Grant-in-aid for Young Scientists (B) (21790207, to R. K.).

[S] The on-line version of this article (available at http://www.jbc.org) contains supplemental Table S1 and S2 and Figs. S1–S5.

All effective genes were submitted to the Gene Expression Omnibus (GEO: ID GSE21560, www.ncbi.nlm.nih.gov).

[1] To whom correspondence should be addressed: Bldg. 37, Rm. 3106, NIH, Bethesda, MD 20892. Tel.: 301-496-0958; Fax: 301-496-8419; E-mail: kimuras@mail.nih.gov.

[2] The abbreviations used are: BLM, bleomycin; SCGB, secretoglobin; CHX, cycloheximide; GO, gene ontology; MMPs, metalloproteinases; qRT, quantitative RT; BALF, bronchoalveolar lavage fluid; αSMA, α smooth muscle actin; rm, recombinant mouse.

fibrosis (5, 6, 12); however, because of potentially harmful side effects, a better alternative is desirable (13).

Secretoglobin (SCGB) 3A2, previously called uteroglobin-related protein 1, is a member of the SCGB gene superfamily (14). The SCGB gene superfamily consists of 3 gene families; family 1 has 4 subfamilies, each composed of 3–11 members, family 2 consists of 2 subfamilies, each with 6–10 members, and family 3 consists of only one subfamily with 5 members (15, 16). All members of the SCGB gene superfamily are cytokine-like secreted proteins of ~10 kDa, found only in mammals. They form homodimers or heterodimers with other members. Most functions of SCGB are still elusive, and the signaling pathways including a possible receptor(s) that transmits activities of these proteins is not known. Among the best studied member of the gene superfamily is SCGB1A1, also called uteroglobin, Clara cell secretory protein, or Clara cell 10-kDa protein that exhibits anti-inflammatory and immunomodulatory activities in lung (17–19). Studies on the mechanisms of the anti-inflammatory activity of SCGB1A1 have been carried out (20, 21). Other members such as SCGB2A2 (mammaglobin A) and SCGB1D2 (lipophilin B) are known as a cancer marker for mammary gland (22) (23).

SCGB3A2 is the second member of the SCGB family 3, subfamily A. It is predominantly expressed in lung airways. SCGB3A2 was found to play a role in suppression of lung inflammation using a mouse model for allergic airway inflammation (24) and to promote branching and maturation of mouse fetal lungs (25). MARCO (macrophage scavenger receptor with collagenous structure), expressed in alveolar macrophages in lung, was suggested as a possible receptor for SCGB3A2 (26). On the other hand, we have demonstrated the possible presence of a SCGB3A2-specific receptor on the mesenchymal cells of mouse fetal lungs (25). Despite these studies, very little is known about the biological and physiological functions of SCGB3A2 and its mechanisms of action including the receptor and the signaling pathway it provokes.

In the present study SCGB3A2 was found to inhibit the TGFβ signaling through increased STAT1 phosphorylation and expression of SMAD7 and decreased phosphorylation of SMAD2/3, thus resulting in inhibition of TGFβ-induced myofibroblast differentiation. In an *in vivo* mouse model, SCGB3A2 markedly suppressed BLM-induced pulmonary fibrosis, suggesting the potential use of SCGB3A2 as a novel therapeutic reagent to treat pulmonary fibrosis.

EXPERIMENTAL PROCEDURES

Isolation and Primary Culture of Lung Fibroblasts—Lung tissues from 7–9-week-old female mice were cut into small pieces, mounted on collagen type I-coated 60-mm plate (IWAKI, Shizuoka, Japan), and then cultured for 7 days. Fibroblasts were harvested by 0.5% trypsin and 0.53 mM EDTA in PBS, washed with DMEM supplemented with 10% FBS, plated on a 35-mm plate, and cultured for 16 h. Fibroblasts were stimulated by 10 ng/ml TGFβ (Sigma) in DMEM containing 3% FBS for 24–72 h in the presence or absence of recombinant mouse (rm) SCGB3A2 (2.5 μg/ml). The recombinant mouse SCGB3A2 (rmSCGB3A2) was purified as described (25) (detailed purification method of SCGB3A2 will be provided upon request). For simplicity "SCGB3A2" is used instead of rmSCGB3A2 throughout the manuscript. For blocking experiments of IFNγ receptor signaling, a specific antibody against IFNγ receptor (rat anti-CD119 clone GR20, BD, Tokyo, Japan) was co-cultured with SCGB3A2 or IFNγ (R & D Systems, Minneapolis, MN) for 24 h or 30 min, respectively. To determine translational regulatory mechanism, fibroblasts were incubated with SCGB3A2 (2.5 μg/ml) and cycloheximide (CHX, 1 μg/ml, WAKO, Osaka, Japan) for 3 h or pretreated with CHX 3 h before stimulation with IFNγ. To down-regulate Stat1 expression, Stat1 siRNA probes (no. 7 probe, sense strand (5′-GCAUCUUACUGAAGGUGAATT-3′) and antisense strand (5′-UUCACCUUCAGUAAGAUGCAT-3′) and no. 8 probe (sense strand 5′-GAGUUGGUUUAAUAUAUAUTT-3′) and antisense strand (5′-AUAUAUAUUAAACCAACUCAT-3′); Qiagen, Valencia, CA) were transfected into fibroblasts using Lipofectamine 2000 (Invitrogen) 48 h before addition of TGFβ and/or SCGB3A2.

Immunoblotting—Immunoblotting was performed using the following antibodies; anti-STAT1, anti-pSTAT1 (Tyr-701), anti-SMAD2, anti-pSMAD2 (Ser-465/467), anti-SMAD3 (Cell Signaling Technology, Danvers, MA), anti-pSMAD3 (Ser-423/425) (Millipore Corp. Temecula, CA), anti-SMAD7 (Santa Cruz Biotechnology, Inc. Santa Cruz, CA), anti-α-smooth muscle actin (αSMA; Sigma), and anti-β-actin (Sigma). Immunoblotting was performed as described in Kurotani *et al.* (25). All immunoreactive bands were visualized using ECL (GE Healthcare) or ImmunoStar LD (WAKO) with LAS-3000mini (FUJIFILM, Tokyo, Japan) and then standardized by immunoreactive band of β-actin using Multi Gauge Version 3.0 software (FUJIFILM).

Quantitative RT-PCR and RT-PCR—Total RNAs isolated using TRIzol (Invitrogen) and digested with DNase I were reverse-transcribed by Superscript II reverse transcriptase (Invitrogen). Quantitative RT-PCR (qRT-PCR) was performed with ABI Prism 7900 Sequence Detection System (Applied Biosystems, Foster City, CA) using SYBR Green master mixture. The standard curve method was used, and all data were normalized to 18 S rRNA amplified using TaqMan Ribosomal RNA Control Reagent, VIC Probe (Applied Biosystems). RT-PCR was performed using AmpliTaq Gold DNA polymerase (Applied Biosystems) with iCycler (Bio-Rad). PCR condition used was 50 °C for 2 min and 95 °C for 10 min followed by 95 °C for 15 s and 60 °C for 40 s for 40 cycles. Primers used for qRT-PCR and RT-PCR analysis are summarized in supplemental Table S1. Leukocytes isolated from normal mouse spleen were stimulated by phorbol 12-myristate 13-acetate, (10 ng/ml) (Calbiochem) and ionomycin (1 μM) (Calbiochem) for 3 h or by poly(I:C) (polyinosinic-polycytidylic acid potassium salt, 10 μg/ml; Imgenex, San Diego, CA) for 24 h. The mRNAs extracted were used as a positive control for IFNγ and IFNα (27) and for IFNβ, respectively (28).

Animals and SCGB3A2 Treatment—C57BL/6N mice (NCI-Frederick, National Institutes of Health) were maintained under a standard 12-h light/12-h dark cycle with water and chow provided *ad libitum*. At least ten 7–8-week-old C57BL/6N mice were prepared for each group. Eight units/kg BLM (Sigma) or PBS was directly administered once by intratracheal intubation into C57BL/6N mice using the BioLITE sys-

tem (BioTex, Inc., Houston, TX). Purified SCGB3A2 (1.5 mg/kg/day) or PBS was intravenously administered to mice via the tail vein once daily for a week starting on day 14 after BLM administration. Four groups of mice were used in this study; administration of BLM followed by intravenous injection of PBS (Group 1) or SCGB3A2 (Group 2) or administration of PBS followed by intravenous injection of PBS (Group 3) or SCGB3A2 (Group 4). All animal studies were performed after approval by the National Cancer Institute Animal Care and Use Committee. SCGB3A2 used in the animal study contained endotoxin at 0.2 enzyme units/mg. The dose of SCGB3A2 was determined based on the previous study in which a total of 200 μg, but not 100 μg, exhibited growth factor activity without causing any gross abnormalities to the dam as well as the embryos (25). For microarray analysis, C57BL/6N mice (7–8 weeks old) were treated with PBS or SCGB3A2 by intravenous administration and were euthanized 12 h later.

Bronchoalveolar Lavage—On day 21 after administration of BLM, mice were euthanized and subjected to bronchoalveolar lavage. Bronchoalveolar lavage fluid (BALF) was obtained by intratracheal instillation of 1 ml of PBS into the lung while it was kept in the thoracic cavity. Cells in the BALF were centrifuged at 500 × *g* and subjected to Diff-Quick (Baxter Healthcare, Miami, FL) staining. Cells were identified and counted using 2000–2500 cells from 10 fields randomly chosen. Tissues were fixed in 4% paraformaldehyde or stored at −80 °C for later RNA preparation.

Pathology—The whole lung was inflated and fixed with 4% paraformaldehyde. Lung tissues were embedded in paraffin, and 4-μm whole lung sections were prepared. Hematoxylin and eosin staining was carried out for assessment of BLM-induced fibrosis. Masson's Trichrome staining (Sigma) was used to detect collagen fibers. Immunohistochemical staining for SCGB3A2, pSMAD2, pSMAD3, and SMAD2/3 was performed in BLM-treated lungs using anti-mouse SCGB3A2 antibody (produced in our laboratory) (14), anti-pSMAD2(ser465/467) (Cell Signaling Technology), anti-pSMAD3 (Epitomics, Burlingame, CA), and anti-SMAD2/3 (BD Biosciences), respectively. For antigen-retrieval, the sections were incubated in Tris-EDTA (pH 6.0) at a temperature over 95 °C for 10 min before protein blocking. The immunoreactivities were enhanced by ABC method (Vector Laboratories, Burlingame, CA) followed by visualization using diaminobenzidine (DakoCytomation, Carpinteria, CA) and counterstained with hematoxylin. Immunocytochemical staining for αSMA was performed as described (29, 30). Briefly, fibroblasts cultured on 8-well Lab Tek Chamber Glass Slide (Nalge Nunc International, Naperville, IL) with and without TGFβ and/or SCGB3A2 were incubated at room temperature in PBS containing 0.1% Triton X 100 for 15 min followed by fixing with 4% paraformaldehyde for 15 min at room temperature. Cells were incubated with anti-αSMA antibody (Sigma, 1:400) overnight at 4 °C after blocking with 3% BSA-PBS for 1 h at room temperature. Cells were incubated with Alexa Fluor 488 goat anti-mouse IgG (Invitrogen) for 30 min at room temperature in dark. Nuclei were stained by 1 mg/ml DAPI (4′,6-diamino-2-phenylindole) (47). The αSMA signal was observed using Nikon EC (Nikon, Tokyo, Japan).

Fibrosis Assessment (Grading)—The grade of BLM-induced pulmonary fibrosis was determined based on the percentage of the fibrotic area in the whole lung section as follows; the presence of fibrosis in 0–25% of the lung for Grade 1, 26–50% of the lung for Grade 2, 51–75% of the lung for Grade 3, and 76–100% of the lung for Grade 4. No fibrosis, but with inflammation including a few infiltrating foci of lymphocytes or a very small granulomas, was considered Grade 0.

DNA Microarray—Total RNAs were purified using TRIzol and RNAeasy (Qiagen, Valencia, CA) from lungs of four groups (Group 1, 2, 3, and 4) of mice as described above or mice 12 h after SCGB3A2 treatment. Ten (group mice analysis) or 20 μg (SCGB3A2 treatment) of purified total RNA were reverse-transcribed to label with Cy3 and Cy5 (GE Healthcare) using the FairPlay Microarray Labeling kit (Stratagene, La Jolla, CA) or SuperScript™ Indirect cDNA Labeling Core kit (Invitrogen), respectively. Microarray analysis was carried out using individually isolated RNA from at least 5 mice in each group and mouse array chips (45K) obtained from the NCI Microarray Facility. Experiments and analysis were performed according to the manufacturer's instruction and the instruction of the Center for Cancer Research, NCI (nciarray.nci.nih.gov). Gene Ontology (GO) analysis (31) and pathway analysis were performed using a mouse gene data (Mm-Std_20060628.gdb) and a mouse pathway data (Mm_Contributed_20070917) from MAPPFinder (32). Up-regulated genes were sorted based on scores (ratio of Cy5 per Cy3) more than 2.0 (average) between Group 1 and Group 3, more than 1.5 (average) between Group1 and Group2, and those up-regulated in all reactions.

Statistical Analysis—Data are shown as the mean ± S.D. from indicated numbers of independent experiments. Statistical analysis was performed one-way ANOVA followed by Bonferroni multiple comparison test.

RESULTS

Effect of SCGB3A2 on Differentiation of Fibroblasts into Myofibroblasts—It was previously demonstrated that SCGB3A2 has at least two biological functions; an anti-inflammatory function was revealed using an ovalbumin-induced allergic airway inflammation model (24), and growth factor activity was studied using *ex vivo* fetal lung organ cultures and *in vivo* injection of SCGB3A2 to pregnant mice (25). To obtain insight into whether SCGB3A2 plays any additional roles in lung physiology and/or diseases, primary fibroblasts obtained from adult mouse lungs were used as an *in vitro* model of fibrosis in which the effect of SCGB3A2 on TGFβ-induced differentiation of fibroblasts into myofibroblasts was studied (33). Inhibition of this transformation would indicate a role for SCGB3A2 in controlling fibrosis. As expected, TGFβ treatment resulted in differentiation of pulmonary fibroblasts to myofibroblasts within 24 h as clearly seen by the characteristic myofibroblast morphology and the robust expression of αSMA (Fig. 1*A*, *TGFβ*, αSMA is seen in *green*). In contrast, treatment of fibroblasts with both TGFβ and SCGB3A2 together (TGFβ+SCGB3A2) exhibited morphology and the level of αSMA expression similar to those of normal fibroblasts (Fig. 1*A*, *Cont. versus TGFβ+SCGB3A2*). SCGB3A2 alone did not have any effect on the morphology of fibroblasts (Fig. 1*A*, *SCGB3A2*). Note that the number of cells

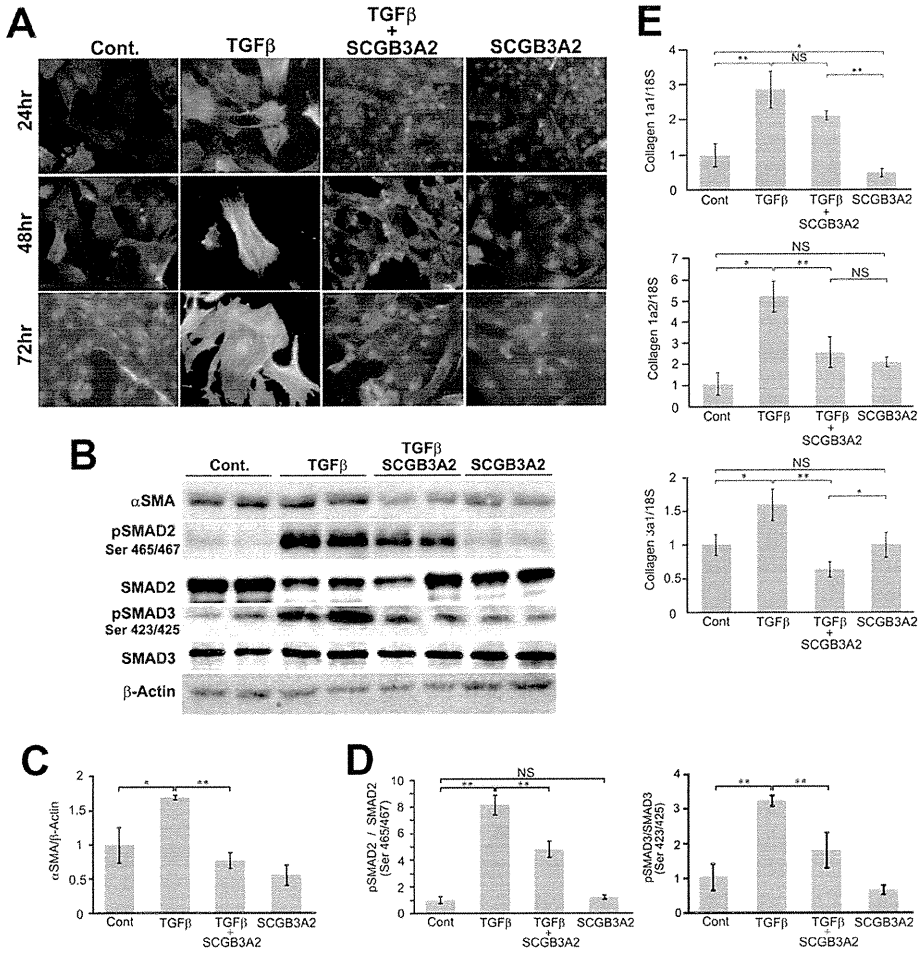

FIGURE 1. **Inhibition of differentiation from fibroblast to myofibroblast by SCGB3A2.** *A*, representative immunocytochemistry for αSMA ($n = 4$) is shown. αSMA was visualized as a *green signal*. Fibroblasts isolated from adult mouse lungs were cultured in the absence (*Cont.*; normal fibroblast) or the presence of SCGB3A2, TGFβ, or TGFβ and SCGB3A2 together for 24–72 h. All the images were taken at ×600 (original magnification). *B*, representative immunoblotting results for αSMA, phosphorylated SMAD2 (*pSMAD2*), total SMAD2, phosphorylated SMAD3 (*pSMAD3*), total SMAD3, and β-actin using cells harvested after 24 h stimulation are shown. *C*, and *D*, densitometric analysis of the immunoblot signals in *B* is shown as the mean ± S.D. ($n = 4$) for αSMA (*C*) and pSMAD2/SMAD2 and pSMAD3/SMAD3 ratios (*D*). *E*, qRT-PCR for collagen 1a1, collagen 1a2, and collagen 3a1 is shown. Fibroblasts were harvested 24 h after stimulation and were subjected to qRT-PCR analysis to determine the level of collagen genes expression. *Cont*, normal fibroblast as control; *TGFβ*, stimulated by TGFβ; *TGFβ+SCGB3A2*, administration of both TGFβ and SCGB3A2; *SCGB3A2*, fibroblast stimulated by SCGB3A2 only. The graph shows the mean ± S.D. from 4–8 lungs per group, each in triplicate. *, $p < 0.05$; **, $p < 0.01$; *NS*, not significant.

did not significantly differ among different culture groups for at least up to 72 h (data not shown). The level of αSMA protein was increased by TGFβ treatment, which returned to control levels in cells treated with SCGB3A2 as determined by Western blotting performed after 24 h of stimulation with TGFβ (Fig. 1, *B* and *C*). SCGB3A2 alone did not have a significant effect on the level of αSMA protein as compared with control. When SMAD2 and SMAD3, the major molecules in the TGFβ signaling pathway, were examined, phosphorylated SMAD2 (*pSMAD2*) and SMAD3 (*pSMAD3*) were increased by TGFβ treatment as expected, and combined treatment with TGFβ and SCGB3A2 partially reversed the increase (Fig. 1, *B* and *D*). Again, SCGB3A2 alone did not have any effect on SMAD2 and SMAD3 phosphorylation. Furthermore, qRT-PCR analysis revealed that the expression of collagen 1a2 and collagen 3a1 was decreased in fibroblasts stimulated by TGFβ and SCGB3A2 together as compared with those treated with TGFβ alone (Fig. 1*E*). Because production of a complete collagen fiber requires three collagens (34), the reduced expression of two collagen genes is likely to account for the reduced Type I and Type III collagen fibers. The effect of SCGB3A2 on the reduced expression of collagen genes was abolished when SCGB3A2 was boiled before the addition to the media, suggesting that the effect of SCGB3A2 was not due to any contaminants in SCGB3A2 preparation (supplemental Fig. S1). These results demonstrated that SCGB3A2 inhibited TGFβ-induced differentiation of primary lung fibroblasts to myofibroblasts.

Induction of STAT1 Phosphorylation and SMAD7 Expression by SCGB3A2—Immunoblotting was performed to examine levels of SMAD7 protein and the status of STAT1 phosphorylation in the presence or absence of TGFβ and/or SCGB3A2 (Fig. 2). It is well documented that IFNγ treatment results in phosphorylation of STAT1 and induces SMAD7 expression, which interferes with the TGFβ signaling (9, 35). In mouse lung primary fibroblasts, the expression of SMAD7, STAT1, and phosphorylated STAT1 was hardly detectable in control and TGFβ-

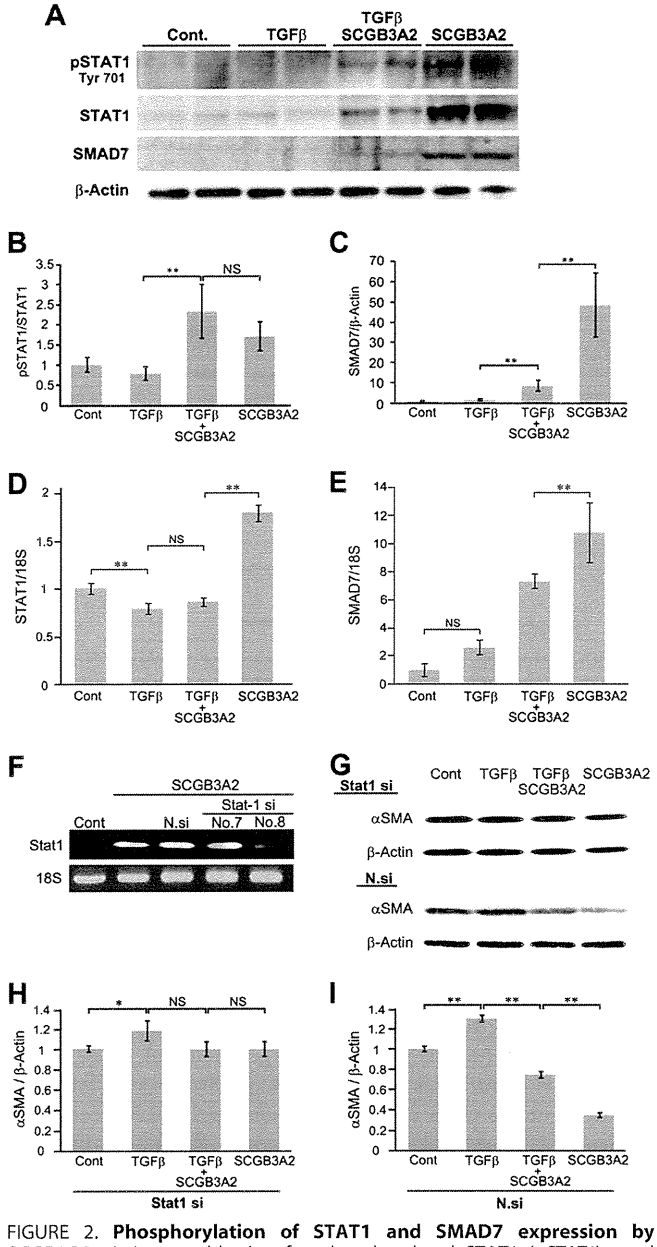

FIGURE 2. **Phosphorylation of STAT1 and SMAD7 expression by SCGB3A2.** *A*, immunoblotting for phosphorylated STAT1 (*pSTAT1*), total STAT1, SMAD7, and β-actin as control is shown. *B* and *C*, shown is a graph for densitometric analysis of the immunoblot signals shown in *A* for pSTAT1/STAT1 (*B*) and SMAD7/β-actin (*C*). The mean ± S.D. ($n = 4$) is shown. *D* and *E*, qRT-PCR for STAT1 (*D*) and SMAD7 (*E*) using 18 S as an internal control is shown. *NS*, not significant. *F–I*, effect of STAT1 siRNA or nonspecific control siRNA on the level of αSMA is shown. *F*, qRT-PCR to confirm knockdown of STAT1 mRNA with STAT1 siRNA probes is shown. *G*, immunoblotting for αSMA and β-actin using cells transfected with no. 8-STAT1 siRNA probe (*STAT1 si*) or nonspecific negative siRNA probe (*N.si*). *H* and *I*, shown is a graph for densitometric analysis of the immunoblot signals shown in *G* for αSMA/β-actin with a STAT1 siRNA probe (*H*) and nonspecific negative siRNA probe (*I*). The mean ± S.D. ($n = 4$) is shown. Fibroblasts were harvested 24 h after stimulation. *Cont*, normal fibroblast as control; *TGFβ*, stimulated by TGFβ; *TGFβ+SCGB3A2*, administration of both TGFβ and SCGB3A2; *SCGB3A2*, fibroblast stimulated by SCGB3A2 only. **, $p < 0.01$, *NS*, not significant. Representative immunoblotting results are shown.

treated cells (Fig. 2*A*). In contrast, the level of STAT1, phosphorylated STAT1 (pSTAT1), and SMAD7 was markedly increased when fibroblasts were treated with SCGB3A2 (Fig. 2, *A–C*). TGFβ dramatically inhibited the induction of STAT1 and SMAD7 by SCGB3A2 (see *TGFβ+SCGB3A2 versus SCGB3A2*), whereas the pSTAT1/STAT1 ratio stayed at similar levels with TGFβ+SCGB3A2 and SCGB3A2-only treatments (Fig. 2*B*). The SCGB3A2-induced increase of STAT1 and SMAD7 expression was due to an mRNA increase as demonstrated by qRT-PCR (Fig. 2, *D* and *E*, respectively). When STAT1 siRNA was transfected to mouse lung primary fibroblasts followed by treatment with TGFβ and/or SCGB3A2, TGFβ-induced αSMA expression levels stayed the same with and without SCGB3A2 (Fig. 2, *G* and *H*). With control nonspecific negative siRNA, TGFβ-induced αSMA expression was reduced by SCGB3A2 as expected (Fig. 2*I*), confirming that the effect of SCGB3A2 is through STAT1. These data demonstrated that SCGB3A2 enhanced expression of SMAD7 and STAT1 and phosphorylation of STAT1, resulting in inhibition of the TGFβ signaling pathway.

Relationship between SCGB3A2 and Interferon γ Receptor—Several cytokines are known to activate STAT1. Among them, the key cytokine that activates STAT1 is IFNγ (36). IFNγ is known to improve fibrosis through phosphorylation of STAT1 (5, 6, 12), and its clinical effect on pulmonary fibrosis is well documented (37). IFNα and IFNβ also activate STAT1 and inhibit fibrosis (38–40). RT-PCR analysis using lung primary fibroblasts demonstrated that IFNγ was not expressed in lung primary fibroblasts regardless of SCGB3A2 treatment (Fig. 3*A*). Similarly, neither IFNα nor IFNβ was expressed in lung primary fibroblasts stimulated by SCGB3A2 (supplemental Fig. S2). In the following studies, we focused on the relationship between SCGB3A2 and IFNγ and its receptor. When IFNγ receptor-specific neutralizing antibody was added to the culture, IFNγ-induced phosphorylation of STAT1 was inhibited, whereas it did not inhibit phosphorylation of STAT1 induced by SCGB3A2 (Fig. 3*B*). Interestingly, it took ~3 h for the SCGB3A2-induced phosphorylation of STAT1 to reach maximum levels (Fig. 3*C*). This was unusually long as compared with the IFNγ-induced STAT1 phosphorylation, which reached maximal levels within 30 min of stimulation (41, 42) (supplemental Fig. S3). Furthermore, SCGB3A2-stimulated STAT1 phosphorylation was suppressed in the presence of CHX (Fig. 3*D*). In contrast, IFNγ-stimulated STAT1 phosphorylation was unchanged with and without CHX treatment (Fig. 3*E*). These data indicated that SCGB3A2 promoted phosphorylation of STAT1 in a manner independent of IFNγ receptor and through a CHX-sensitive intermediate molecule. These data further suggested that the SCGB3A2-STAT1 signaling may have been through a SCGB3A2-specific receptor.

Inhibition of BLM-induced Lung Fibrosis by SCGB3A2—To validate these *in vitro* data that SCGB3A2 suppresses the TGFβ signaling pathway resulting in reduction of fibrosis, mice were subjected to a pulmonary fibrosis model. Pulmonary fibrosis was induced by direct administration of BLM or PBS as control to mice by intratracheal intubation. The histopathology of the lungs on day 14 (2 weeks) after BLM treatment did not reveal any fibrosis regardless of treatment regimens (data not shown). At day 14, mice received the first of 7 daily consecutive intravenous injections of SCGB3A2 or PBS through the tail vein (Fig. 4*A*). On day 21 after BLM administration, pulmonary fibrosis

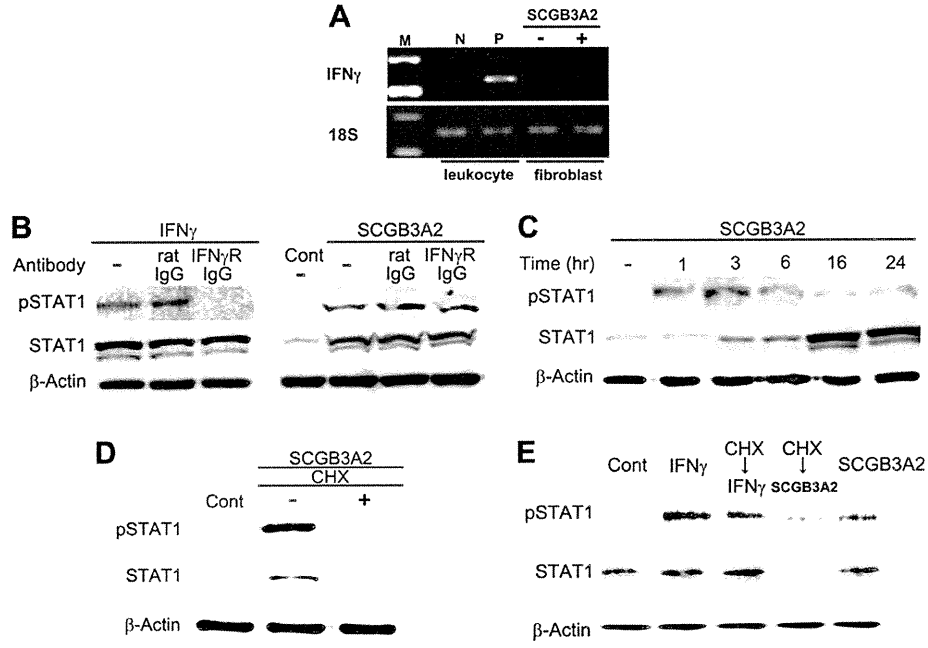

FIGURE 3. **Relationship between SCGB3A2 and IFNγ receptor.** *A*, representative RT-PCR for IFNγ in fibroblasts in the presence or absence of SCGB3A2 (n = 3) is shown. Leukocytes stimulated by phorbol 12-myristate 13-acetate (10 ng/ml) and ionomycin (1 μM) for 3 h were used as a positive control for IFNγ. *B*, shown are blocking experiments for IFNγ receptor signaling. A representative result is shown (n = 3). pSTAT1 was detected in the presence of anti-IFNγ receptor antibody and SCGB3A2 (*right panel*). *C*, a representative time-course result of STAT1 phosphorylation by SCGB3A2 (n = 3) is shown. *D* and *E*, protein synthesis blocking experiments are shown. Fibroblasts were incubated with both SCGB3A2 and CHX (1 μg/ml) for 3 h (*D* and *E* for CHX→SCGB3A2) or were preincubated with CHX (1 μg/ml) for 3 h before stimulation with IFNγ for 15 min (*E*). A representative result is shown (n = 3).

was observed in the lungs of BLM-treated group of mice (Group 1). The extent of fibrosis was rated as grade 1 to grade 2 (Fig. 4*B*). In contrast, mice in Group 2 that received BLM and SCGB3A2 did not develop any pulmonary fibrosis except one mouse of five tested. In Group 3, one mouse exhibited small fibrotic lesions, whereas no fibrosis was observed in Group 4 mice. Collagen fibers were found to focally occupy the alveolar space of mice in Group 1 but not in other groups of lungs as determined by Masson's Trichrome staining, which detects collagen fibers (Fig. 4*C*, *upper panel*). Excessive SCGB3A2 expression was focally found in a part of airway epithelial cells and the foci of fibrosis of Group 1 mouse lungs (Fig. 4*C*, *lower panel*). In contrast, other groups of lungs (Groups 2–4) expressed SCGB3A2 at similar levels in airway epithelial cells as expected, although Group 2 lungs appeared to have slightly higher expression than Group 3 and 4 lungs. When the expression of total SAMD2/3 as well as pSMAD2 and pSMAD3 was examined by immunohistochemistry, all were highly up-regulated in most of airway epithelial cells as well as the foci of fibrosis in Group 1 mouse lungs, whereas expression stayed at similar levels and patterns in other groups of lungs including those of BLM+SCGB3A2 administered mouse lungs (Group 2) (supplemental Fig. S4). The latter results suggested that SCGB3A2 appeared to have suppressed expression of SMAD2/3 and/or pSMAD2 and pSMAD3 in epithelial as well as parenchymal cells. The numbers of macrophages and neutrophils in BALF were enhanced by BLM treatment, whereas they were markedly reduced to levels close to that of controls in the SCGB3A2-treated group (Fig. 4*D*). The number of lymphocytes was not different with statistical significance among the four groups (data not shown). These data indicated that development of BLM-induced fibrosis was suppressed by the daily administration of SCGB3A2 on the third week of BLM treatment.

Alteration of Gene Expression by BLM and/or SCGB3A2—To determine the genes whose expression was altered in the BLM-induced lung fibrosis and/or SCGB3A2-induced reduction of fibrosis, microarray analysis was carried out using mRNAs obtained from lungs of mice between Group 1 (BLM-treated) and Group 3 (PBS control) and Group 1 (BLM-treated) and Group 2 (BLM- and SCGB3A2-treated). With a cutoff of >1.5-fold change in expression, 1646 and 1275 genes were, respectively, up- and down-regulated by BLM as compared with control PBS (between Group 1 and Group 3), and 346 and 919 genes were, respectively, up- and down-regulated by SCGB3A2 treatment as compared with no SCGB3A2 treatment in BLM treated mice (between Group 1 and Group 2). Using these genes, GO (gene ontology) analysis was performed for the changes caused by BLM and for the effect of SCGB3A2 in BLM-treated mice (heat map results are shown in supplemental Fig. S5). The results revealed that "Inflammatory response" and "Response to wounding" under "Biological Process" and "Extracellular region part," "Extracellular region," and "Extracellular space" under "Cellular Component" were overexpressed by BLM injury (Table 1) and suppressed by administration of SCGB3A2 (Table 2). Additionally, to demonstrate genes that are altered by SCGB3A2, microarray analysis was carried out using lung RNAs of normal mice that were intravenously administered SCGB3A2 and were euthanized 12 h later. GO analysis revealed that "Signal transducer activity" and "Molec-